# Distributed State Estimation for Renewable Energy Microgrids with Sensor Saturations ⋆

Bogang Qu [a,c], Zidong Wang [b], Bo Shen [a,c,*], Hongli Dong [d]

[a] College of Information Science and Technology, Donghua University, Shanghai 201620, China

[b] Department of Computer Science, Brunel University London, Uxbridge, Middlesex, UB8 3PH, United Kingdom

[c] Engineering Research Center of Digitalized Textile and Fashion Technology, Ministry of Education, Shanghai 201620, China

[d] Institute of Artificial Intelligence Energy, Northeast Petroleum University, Daqing 163318, China

**Abstract**

In this paper, the distributed state estimation problem is studied for renewable energy microgrids with sensor saturations. A system model for the microgrids with sensor saturations is proposed. Attention is focused on the design of a distributed recursive estimation scheme such that, in the presence of the sensor saturations, an upper bound of the estimation error covariance is guaranteed. Subsequently, such an upper bound is minimized by appropriately designing the gain matrices of the corresponding state estimator. In particular, the sparsity of the gain matrices resulting from network topology is handled by using a matrix simplification method. Moreover, the performance evaluation of the designed distributed state estimator is conducted by analyzing the exponential boundedness of the estimation error in the mean square sense. Finally, simulation experiments under two cases are carried out on a renewable energy microgrid which contains two distributed generation units. The simulation results demonstrate that the developed state estimation scheme is effective.

*Key words:* Microgrid; Sensor saturations; Power systems; Distributed state estimation; Recursive state estimation.

## 1 Introduction

Most of the electrical power that we consume today comes from fossil-fuel power plants and these plants have quite low efficiency in generating power while emitting lots of carbon dioxide into the air [37]. As a kind of clean yet environmentally friendly process for electricity generation, the renewable energy generation has recently attracted considerable research attention [5, 7, 20]. Nevertheless, with the increasing share of the electricity produced by renewable energy, the conventional power system cannot be fully integrated with diversified renewable energy generation. In order to handle such a challenge and minimize the number of fossil-fuel power plants that need to be built, a new power generation infrastructure, namely, smart grid, has been put forward in electricity industry, which facilitates the easy integration of the renewable energy microgrid (REM) into the main power grid [17, 37].

It is worth mentioning that the nowadays popular REM may give rise to a certain degree of uncertainties and/or dynamics with the power system primarily due to unpredictable weather conditions [12, 40]. As such, it is critically important to monitor the REM in a robust yet dynamical way, especially when the REM is integrated into the main power grid. On the other hand, knowing the system states is also a prerequisite for operating basic functionalities of the microgrid and acting feedback signals [18]. It is, therefore, an essential mission to estimate the system states with hope to ensure that the microgrid operates in a normal yet secure manner [10, 12, 17].

Since the initial research conducted in the early 1970s [34], the state estimation (SE) method based on the weighted-least-square (WLS) technique has been widely studied and applied in power systems due to the properties of easy implementation and reliable capability [10, 16, 17]. It is worthwhile to note that the WLS-based algorithm is performed at regular but relatively long intervals under the assumption that the power system evolves in the quasi-steady condition [12, 16]. The renewable energy resources, which may inject uncertainties and/or dynamics into the power systems, clearly violate the assumption mentioned above [1, 12]. Moreover, the high resistance-to-reactance ratios, unbalanced phase and non-ideal measurements which, in turn, also limit the application scope of the WLS-based SE method [1, 17]. Furthermore, the WLS-based SE algorithm can only forecast the current system states while cannot generate the estimates for the next time step [16]. As such, there is a practical need to develop new SE schemes, which are accurate, sustainable and easy-to-implement, for dynamical REMs in response to the ever-increasing demand for green electricity generation processes.

State estimation has long been a fundamental research topic in the areas of signal process and control engineer-

⋆ This work was supported in part by the National Natural Science Foundation of China under Grants 61873059, 61873148, 61922024, 61933007 and 61873058, the Program of Shanghai Academic/Technology Research Leader of China under Grant 20XD1420100, the Natural Science Foundation of Shanghai of China under Grant 18ZR1401500, the Natural Science Foundation of Heilongjiang Province of China under Grant ZD2019F001, the Fundamental Research Funds for the Central Universities and Graduate Student Innovation Fund of Donghua University of China under Grant CUSF-DH-D-2021046, and the Alexander von Humboldt Foundation of Germany.

* Corresponding author.

*Email addresses:* bogangqu@163.com (Bogang Qu), Zidong.Wang@brunel.ac.uk (Zidong Wang), bo.shen@dhu.edu.cn (Bo Shen), shiningdhl@vip.126.com (Hongli Dong).

ing [2–4, 9, 24, 26, 42–45]. In recent years, the distributed state estimation (DSE) problems have gained a particular interest from many researchers [15, 25, 32, 36, 38]. Compared with the centralized SE approach, the communication and computation burden of the distributed one is much lower since the SE is performed in a parallel manner [6, 23, 25, 39]. Moreover, the fault-tolerant capability is improved since the high risk of the single point failure is avoided [39]. Furthermore, the deviations of the estimates caused by the uncertainties and/or dynamics of the REMs can be compensated by using the neighboring sensing information. Up to now, fruitful results concerning the DSE problem for the conventional power systems have been proposed, see e.g. [16, 17]. When it comes to the microgrids, the relevant results have been very few except the *scattered* results reported in [8, 11]. For instance, in [11], the optimal zone clustering algorithm has been proposed for the microgrid and the DSE issue has been considered in the design of such an algorithm. In [8], the operation and protection scheme for the microgrids has been studied by using the DSE technique, while the state estimator is a WLS-based one. As such, there is a lack of adequate research on the design of the DSE scheme for microgrids, and this constitutes one of the motivations of this paper.

As the fundamental components of the sensors in power systems, the instrument transformers (e.g. current transformers and phase voltage transformers) play a vital role in the connections between the power systems and the measuring facilities such as the remote terminal units (RTUs) and the phasor measurement units (PMUs) [22, 41]. However, these transformers may be saturated due to the transient processes, electrical faults or highly overloaded lines [14]. Moreover, the extreme weather or working conditions may also saturate the sensor [22]. It is worth noting that the typical nonlinear phenomenon caused by the sensor saturations may result in bad measurements and further affect the online control or protection of the power systems if not handled appropriately [19, 41]. In the past decades, the SE problem with sensor saturations has received considerable research attention [27, 28, 35]. Nevertheless, when it comes to the microgrids, most of the results rely on the assumption that the measurements are ideal, see e.g. [11, 12, 32] and the references therein. Therefore, it constitutes another motivation for us to tackle the SE problem for microgrids in the context of sensor saturations.

Motivated by the above discussions, it can be concluded that there is a lack of systematic investigation on the distributed SE problem for microgrids suffering from sensor saturations. As such, the main purpose of this paper is to propose distributed recursive SE algorithms for a class of REMs such that, in the presence of sensor saturations, an upper bound of the estimation error covariance is guaranteed and subsequently minimized at each time instant by properly designing the state estimator gains. The main novelties of this paper can be highlighted as follows: *1) the SE problem is, for the first time, investigated for REMs with sensor saturations; 2) a distributed recursive SE method is developed to estimate the state of the microgrid in the presence of sensor saturations, which is computationally efficient yet suitable for online application; and 3) a sufficient criterion is given to guarantee the exponential boundedness of the estimation error.*

**Notation** The notation used here is fairly standard except where otherwise stated. $I_n$ represents the identity matrix of $n$ rows and $n$ columns. For $i = 1, 2, \ldots, n$, $\mathrm{diag}_n\{A_i\}$ stands for a block-diagonal matrix where the square matrices $A_i$ are the corresponding diagonal blocks, and $\mathrm{col}_n\{x_i\}$ stands for the vector $[x_1^T, \cdots, x_n^T]^T$.

## 2 Problem Formulation

### 2.1 Preliminaries

In this paper, a sensor network consisting of $n$ sensor nodes is used to monitor the microgrid. We denote the topology of the network by a directed graph $\mathcal{G} = (\mathcal{V}, \mathcal{E}, \mathcal{A})$ of order $n$ with the set of nodes $\mathcal{V} = \{1, 2, \ldots, n\}$, the set of edges $\mathcal{E} \in \mathcal{V} \times \mathcal{V}$, and the weighted adjacency matrix $\mathcal{A} = [a_{ij}]$ with nonnegative elements $a_{ij}$. An edge of $\mathcal{G}$ is denoted by ordered pair $(i, j)$. The adjacency elements associated with the edges of the graph are positive, i.e., $a_{ij} > 0 \Longleftrightarrow (i, j) \in \mathcal{E}$, which means that the $i$-th node can receive the information from the $j$-th node. Also, we assume that $a_{ii} = 1$ for all $i \in \mathcal{V}$. The set of neighbors of node $i$ plus the node itself are denoted by the set as $N_i = \{i \in \mathcal{V} : (i, j) \in \mathcal{E}\}$.

### 2.2 System Model of Renewable Energy Microgrid

A typical REM which contains two distributed generation (DG) units is shown in Fig. 1. In each DG unit, the renewable energy sources are modeled as dc voltage sources, and the voltage source converter (VSC) with a series filter is connected to one side of the step-up transformer, and the other side of the step-up transformer is connected to the point of common coupling (PCC) and the load. Then each DG unit is connected to the transmission line through the PCC. It is assumed that the REM is operating under balanced conditions. Applying Kirchhoff's laws and Park's transformation, the state-space model of *abc*-frame can be transferred into a rotating *dq*-frame with the microgrid frequency of $\omega_0$ [33]:

$$\text{DG } r: \begin{cases} \dot{V}_r^{dq} = -j\omega_0 V_r^{dq} + \dfrac{d_r}{C_r} I_{tr}^{dq} + \dfrac{I_{rs}^{dq}}{C_r}, \\ \dot{I}_{tr}^{dq} = -j\omega_0 I_{tr}^{dq} - \dfrac{d_r}{L_{tr}} V_r^{dq} - \dfrac{R_{tr}}{L_{tr}} I_{tr}^{dq} + \dfrac{V_{tr}^{dq}}{L_{tr}}, \end{cases} \tag{1a}$$

$$\text{Line } rs: \begin{cases} \dot{I}_{rs}^{dq} = -j\omega_0 I_{rs}^{dq} + \dfrac{V_s^{dq}}{L_{rs}} - \dfrac{R_{rs}}{L_{rs}} I_{rs}^{dq} - \dfrac{V_r^{dq}}{L_{rs}}, \end{cases} \tag{1b}$$

$$\text{DG } s: \begin{cases} \dot{V}_s^{dq} = -j\omega_0 V_s^{dq} + \dfrac{d_s}{C_s} I_{ts}^{dq} + \dfrac{I_{sr}^{dq}}{C_s}, \\ \dot{I}_{ts}^{dq} = -j\omega_0 I_{ts}^{dq} - \dfrac{d_s}{L_{ts}} V_s^{dq} - \dfrac{R_{ts}}{L_{ts}} I_{ts}^{dq} + \dfrac{V_{ts}^{dq}}{L_{ts}}, \end{cases} \tag{1c}$$

$$\text{Line } sr: \begin{cases} \dot{I}_{sr}^{dq} = -j\omega_0 I_{sr}^{dq} + \dfrac{V_r^{dq}}{L_{sr}} - \dfrac{R_{sr}}{L_{sr}} I_{rs}^{dq} - \dfrac{V_s^{dq}}{L_{sr}}, \end{cases} \tag{1d}$$

where $(V_r^{dq}, V_s^{dq})$, $(V_{tr}^{dq}, V_{ts}^{dq})$, $(I_{tr}^{dq}, I_{ts}^{dq})$ and $(I_{rs}^{dq}, I_{sr}^{dq})$ are, respectively, *dq* components of PCC voltages, VSC terminal voltages, series filter currents and transmission

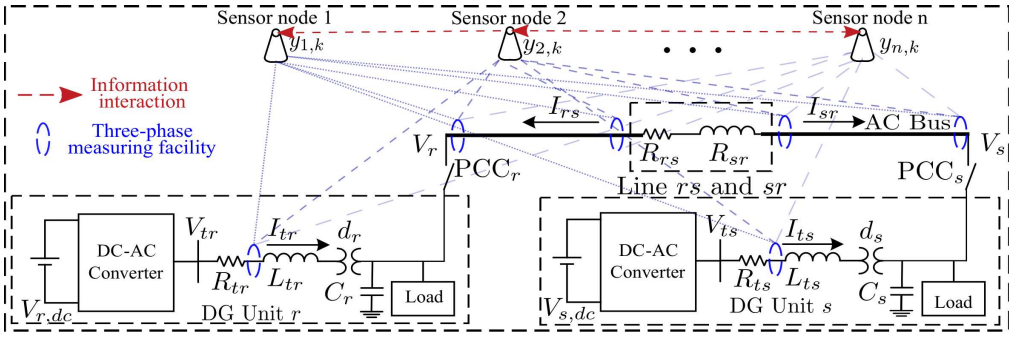


Fig. 1. Diagram of the distributed state estimation for the renewable energy microgrid.

line currents of DG unit $r$ and $s$. In this case, the state-space model of the microgrid can be constructed as

$$\dot{x} = Ax + Bu \tag{2}$$

where $x = [V_r^d \ V_r^q \ I_{tr}^d \ I_{tr}^q \ I_{rs}^d \ I_{rs}^q \ I_{sr}^d \ I_{sr}^q \ V_s^d \ V_s^q \ I_{ts}^d \ I_{ts}^q]^T \triangleq [x_1 \ \ x_2 \ \cdots \ x_{12}]^T \in \mathbb{R}^{n_x}$ is the state vector and $u = [V_{tr}^d \ V_{tr}^q \ V_{ts}^d \ V_{ts}^q]^T \triangleq [u_1 \ \ u_2 \ \ u_3 \ \ u_4]^T \in \mathbb{R}^{n_u}$ is the known input vector. The matrices $A$ and $B$ can be obtained by referring to [33].

Discretizing the system (2) with a period $\Delta t$, we obtain the discretized model as follows:

$$x_{k+1} = A_d x_k + B_d u_k + w_k \tag{3}$$

where $A_d = e^{A\Delta t}$ and $B_d = \int_0^{\Delta t} e^{A\Delta t} B dt$, $u_k$ is the known input vector after discretization, and $w_k \in \mathbb{R}^{n_x}$ is a zero mean Gaussian sequence with covariance $W_k > 0$ that accounts for any modeling error. The initial state $x_0$ is a random variable with mean $\eta_0$ and covariance $\Sigma_{0|0}$.

### *2.3 Distributed State Estimator for Renewable Energy Microgrid with Sensor Saturations*

A schematic overview of the DSE for the microgrid is given in Fig. 1. Specifically, for DG unit $r$ and $s$, the $abc$ components of PCC voltages $(V_r^{abc}, V_s^{abc})$, series filter currents $(I_{tr}^{abc}, I_{ts}^{abc})$ and transmission line currents $(I_{rs}^{abc}, I_{sr}^{abc})$ are all measured. Note that, for every sensor node, the specific measuring items are usually different. As such, for sensor node $i$ $(1 \le i \le n)$, we use a general expression to model the measurement with sensor saturation as follows:

$$y_{i,k} = \sigma_i(C_{i,k} x_k) + v_{i,k} \tag{4}$$

where $y_{i,k} \in \mathbb{R}^{m_i}$ is the measurement output received by the sensor node $i$ from microgrid, $C_{i,k} \in \mathbb{R}^{m_i \times n_x}$ is a known matrix, and $v_{i,k} \in \mathbb{R}^{m_i}$ is the Gaussian measurement noise with zero mean and covariance $R_{i,k} > 0$. Throughout this paper, we assume that $w_k$, $v_{i,k}$ and $x_0$ are mutually independent.

The saturation function $\sigma_i(\cdot) : \mathbb{R}^{m_i} \to \mathbb{R}^{m_i}$ for every sensor node $i$ $(1 \le i \le n)$ is defined as

$$\sigma_i(r_i) = \left[\sigma_i^1(r_i^1) \ \ \sigma_i^2(r_i^2) \ \ \cdots \ \ \sigma_i^{m_i}(r_i^{m_i})\right]^T \tag{5}$$

with

$$\sigma_i^s(r_i^s) \triangleq \text{sign}(r_i^s) \min\{r_{i,\max}^s, |r_i^s|\}, \quad s = 1, 2, \cdots, m_i$$

where $\text{sign}(\cdot)$ is the signum function and $r_{i,\max}^s$ (i.e., the saturation level) is the $s$th element of the vector $r_{i,\max}$.

**Remark 1** *In order to characterize the relationship between the measurable electrical signals in the abc-frame and the state variables in the dq-frame, the inverse Park's transformation are utilized in this paper [21]. Specifically, suppose that the abc components of a three-phase AC signal can be measured (i.e., $y_k = [V_k^a \ V_k^b \ V_k^c]^T$), then the relationship between the measured components and the state variables in the dq-frame (i.e., $x_k = [V_k^d \ V_k^q]^T$) can be characterized as $y_k = \mathscr{C}_k x_k$ with*

$$\mathscr{C}_k = \begin{bmatrix} \cos(\theta_k) & -\sin(\theta_k) \\ \cos(\theta_k - \frac{2}{3}\pi) & -\sin(\theta_k - \frac{2}{3}\pi) \\ \cos(\theta_k + \frac{2}{3}\pi) & -\sin(\theta_k + \frac{2}{3}\pi) \end{bmatrix}$$

*where $\theta_k = \omega_0 k$. Note that, in power systems, it is a common approach to measure at least two components of a three-phase AC signal. As such, the sensing matrix $C_{i,k}$ relies on the measuring components we choose. Actually, the voltages and currents are very essential measuring items in power systems, and some additional measurements (e.g. active and reactive power injections) are all relying on the measurements of voltages and currents.*

In this paper, a recursive state estimator is designed as follows:

$$\hat{x}_{i,k|k-1} = A_d \hat{x}_{i,k-1|k-1} + B_d u_{k-1}, \tag{6}$$

$$\hat{x}_{i,k|k} = \hat{x}_{i,k|k-1} + \sum_{j \in N_i} a_{ij} G_{ij,k} \tilde{y}_{j,k} \tag{7}$$

with the initial value $\hat{x}_{i,0|0} = \mathbb{E}[x_0] = \eta_0$, where $\hat{x}_{i,k|k-1}$ and $\hat{x}_{i,k|k}$ are the one-step prediction and the estimate of state vector $x_k$, respectively, $\tilde{y}_{j,k} = y_{j,k} - C_{j,k}\hat{x}_{j,k|k-1}$ is the innovation sequence, and $G_{ij,k} \in \mathbb{R}^{m_x \times m_j}$ are the state estimator gain matrices to be designed.

**Remark 2** *Similar with [25], the distributed state estimator presented in* (6) *and* (7) *follows the well-known prediction-correction paradigm. The difference is that we have to meet the specified performance requirements by using the available information of the saturated sensors in the following state estimator design.*

For node $i$, the one-step prediction error $e_{i,k|k-1} \triangleq x_k - \hat{x}_{i,k|k-1}$ and the estimation error $e_{i,k|k} \triangleq x_k - \hat{x}_{i,k|k}$ can be written as

$$e_{i,k|k-1} = A_d e_{i,k-1|k-1} + w_{k-1}, \tag{8}$$

$$e_{i,k|k} = e_{i,k|k-1} - \sum_{j\in N_i} a_{ij}G_{ij,k}\tilde{y}_{j,k}. \tag{9}$$

For sake of simplicity, we denote

$$\begin{aligned}
e_{k|k-1} &\triangleq \mathrm{col}_n\{e_{i,k|k-1}\}, \quad e_{k|k} \triangleq \mathrm{col}_n\{e_{i,k|k}\},\\
\bar{x}_k &\triangleq \mathrm{col}_n\{x_k\}, \quad \hat{x}_{k|k-1} \triangleq \mathrm{col}_n\{\hat{x}_{i,k|k-1}\},\\
\hat{x}_{k|k} &\triangleq \mathrm{col}_n\{\hat{x}_{i,k|k}\}, \quad \bar{w}_k \triangleq \mathrm{col}_n\{w_k\},\\
\bar{v}_k &\triangleq \mathrm{col}_n\{v_{i,k}\}, \quad G_k \triangleq \{G_{ij,k}\}_{n\times n},\\
H_i &\triangleq \mathrm{diag}\{a_{i1}I_{m_1},\cdots,a_{in}I_{m_n}\}, \quad \bar{A} \triangleq \mathrm{diag}_n\{A_d\},\\
\bar{C}_k &\triangleq \mathrm{diag}_n\{C_{i,k}\}, \quad \sigma(\bar{C}_k\bar{x}_k) \triangleq \mathrm{col}_n\{\sigma_i(C_{i,k}x_k)\},\\
E_i &\triangleq \mathrm{diag}\{\underbrace{0,\cdots,0}_{i-1}, I_{n_x}, \underbrace{0,\cdots,0}_{n-i}\}.
\end{aligned}$$

Furthermore, by denoting $K_k \triangleq \sum_{i=1}^{n} E_iG_kH_i$, the one-step prediction error $e_{k|k-1} \in \mathbb{R}^{n\times n_x}$ and the estimation error $e_{k|k} \in \mathbb{R}^{n\times n_x}$ can be rewritten in a compact form as

$$e_{k|k-1} = \bar{A}e_{k-1|k-1} + \bar{w}_k, \tag{10}$$

$$\begin{aligned}
e_{k|k} =&(I - K_k\bar{C}_k)e_{k|k-1} + K_k\bar{C}_k\bar{x}_k\\
&- K_k\sigma(\bar{C}_k\bar{x}_k) - K_k\bar{v}_k.
\end{aligned} \tag{11}$$

Define the one-step prediction error covariance $P_{k|k-1} \triangleq \mathbb{E}\{e_{k|k-1}e_{k|k-1}^T\}$ and the estimation error covariance $P_{k|k} \triangleq \mathbb{E}\{e_{k|k}e_{k|k}^T\}$. The objective of this paper is to design a state estimator of the form (6) and (7) such that there exists an upper bound on the estimation error covariance $P_{k|k}$ and such an upper bound is minimized at each time instant by appropriately designing the estimator gains.

## 3 Main Results

**Lemma 1** *[39] For matrices $X, Y$ and a positive scalar $\lambda$, the following inequality holds:*

$$XY^T + YX^T \le \lambda XX^T + \lambda^{-1}YY^T.$$

**Lemma 2** *[43] For matrices $M$, $N$, $X$ and $K$ with appropriate dimensions, the following equations hold*

$$\frac{\partial \mathrm{tr}(MKN)}{\partial K} = M^TN^T,$$

$$\frac{\partial \mathrm{tr}[(MKN)P(MKN)^T]}{\partial K} = 2M^TMKNPN^T.$$

### 3.1 Estimator Design

From (10), the one-step prediction error covariance $P_{k|k-1}$ is calculated as

$$P_{k|k-1} = \bar{A}P_{k|k}\bar{A}^T + \bar{W}_k \tag{12}$$

with $\bar{W}_k = \mathbb{E}\{\bar{w}_k\bar{w}_k^T\}$. Subsequently, in view of (11), we can obtain the recursion of the estimation error covariance, which is shown in the following lemma.

**Lemma 3** *The recursion of the estimation error covariance $P_{k|k}$ can be obtained as follows:*

$$\begin{aligned}
P_{k|k} =&\Theta_kP_{k|k-1}\Theta_k^T + K_k\bar{C}_k\mathbb{E}\{\bar{x}_k\bar{x}_k^T\}\bar{C}_k^TK_k^T\\
&+ K_k\mathbb{E}\{\sigma(\bar{C}_k\bar{x}_k)\sigma^T(\bar{C}_k\bar{x}_k)\}K_k^T + \mathcal{F}_{1,k} + \mathcal{F}_{1,k}^T\\
&+ \mathcal{F}_{2,k} + \mathcal{F}_{2,k}^T + \mathcal{F}_{3,k} + \mathcal{F}_{3,k}^T + K_kR_kK_k^T
\end{aligned} \tag{13}$$

*with*

$$\begin{aligned}
\Theta_k &= I - K_k\bar{C}_k,\ R_k = \mathrm{diag}_n\{R_{i,k}\},\\
\mathcal{F}_{1,k} &= \mathbb{E}\{\Theta_ke_{k|k-1}\bar{x}_k^T\bar{C}_k^TK_k^T\},\\
\mathcal{F}_{2,k} &= \mathbb{E}\{-\Theta_ke_{k|k-1}\sigma^T(\bar{C}_k\bar{x}_k)K_k^T\},\\
\mathcal{F}_{3,k} &= \mathbb{E}\{-K_k\bar{C}_k\bar{x}_k\sigma^T(\bar{C}_k\bar{x}_k)K_k^T\}.
\end{aligned}$$

*Proof:* It follows from (11) that

$$\begin{aligned}
P_{k|k} =&\Theta_kP_{k|k-1}\Theta_k^T + \Theta_k\mathbb{E}\{e_{k|k-1}\bar{x}_k^T\}\bar{C}_k^TK_k^T\\
&+ K_k\bar{C}_k\mathbb{E}\{\bar{x}_ke_{k|k-1}^T\}\Theta_k^T\\
&- \Theta_k\mathbb{E}\{e_{k|k-1}\sigma^T(\bar{C}_k\bar{x}_k)\}K_k^T\\
&- K_k\mathbb{E}\{\sigma(\bar{C}_k\bar{x}_k)e_{k|k-1}^T\}\Theta_k^T\\
&+ K_k\bar{C}_k\mathbb{E}\{\bar{x}_k\bar{x}_k^T\}\bar{C}_k^TK_k^T\\
&- K_k\bar{C}_k\mathbb{E}\{\bar{x}_k\sigma^T(\bar{C}_k\bar{x}_k)\}K_k^T\\
&- K_k\mathbb{E}\{\sigma(\bar{C}_k\bar{x}_k)\bar{x}_k^T\}\bar{C}_k^TK_k^T\\
&+ K_k\mathbb{E}\{\sigma(\bar{C}_k\bar{x}_k)\sigma^T(\bar{C}_k\bar{x}_k)\}K_k^T\\
&+ K_k\mathbb{E}\{\bar{v}_k\bar{v}_k^T\}K_k^T - \mathcal{L}_{1,k} - \mathcal{L}_{1,k}^T\\
&- \mathcal{L}_{2,k} - \mathcal{L}_{2,k}^T + \mathcal{L}_{3,k} + \mathcal{L}_{3,k}^T
\end{aligned}$$

where

$$\begin{aligned}
\mathcal{L}_{1,k} &= \mathbb{E}\{\Theta_ke_{k|k-1}\bar{v}_k^TK_k^T\},\\
\mathcal{L}_{2,k} &= \mathbb{E}\{K_k\bar{C}_k\bar{x}_k\bar{v}_k^TK_k^T\},\\
\mathcal{L}_{3,k} &= \mathbb{E}\{K_k\sigma(\bar{C}_k\bar{x}_k)\bar{v}_k^TK_k^T\}.
\end{aligned}$$

Moreover, it is obvious that

$$\mathbb{E}\{\bar{v}_k\bar{v}_k^T\} = \mathrm{diag}_n\{R_{i,k}\} = R_k.$$

Noting that the one-step prediction error $e_{k|k-1}$ is uncorrelated with $\bar{v}_k$, $\mathcal{L}_{1,k}$ vanishes. Also, using the fact that $\bar{v}_k$ is uncorrelated with $\bar{x}_k$ and $\sigma(\bar{C}_k\bar{x}_k)$, one derives that $\mathcal{L}_{2,k} = 0$ and $\mathcal{L}_{3,k} = 0$. The proof is complete.

**Theorem 1** *For positive scalars $\lambda_{i,k}$ $(i = 1, 2, 3, 4)$, assume that there exist symmetric positive-definite solutions $M_{k|k-1} \in \mathbb{R}^{nn_x\times nn_x}$ and $M_{k|k} \in \mathbb{R}^{nn_x\times nn_x}$ to the following difference equations:*

$$M_{k|k-1} = \bar{A}M_{k-1|k-1}\bar{A}^T + \bar{W}_{k-1} \tag{14}$$

*and*

$$\begin{aligned}
M_{k|k} =&(1 + \lambda_{1,k} + \lambda_{2,k})\Theta_kM_{k|k-1}\Theta_k^T\\
&+ (1 + \lambda_{1,k}^{-1} + \lambda_{3,k})K_k\bar{C}_k\Phi_k\bar{C}_k^TK_k^T\\
&+ K_k\big[\bar{r}(1 + \lambda_{2,k}^{-1} + \lambda_{3,k}^{-1})I + R_k\big]K_k^T
\end{aligned} \tag{15}$$

*with the initial condition $M_{0|0} = P_{0|0}$, where*

$$\begin{aligned}
\Phi_k &= (1 + \lambda_{4,k})M_{k|k-1} + (1 + \lambda_{4,k}^{-1})\mathbb{E}\{\hat{x}_{k|k-1}\hat{x}_{k|k-1}^T\},\\
\bar{r} &= \sum_{i=1}^{n}\sum_{j=1}^{m_i}(r_{i,\max}^j)^2.
\end{aligned}$$

*Then, the matrix $M_{k|k}$ is an upper bound of $P_{k|k}$, i.e.,*

$$P_{k|k} \le M_{k|k}. \tag{16}$$

*Proof:* First, let us handle the right-hand side of (13) term by term. By using Lemma 1, the unknown terms $\mathcal{F}_{1,k}, \mathcal{F}_{2,k}$ and $\mathcal{F}_{3,k}$ in (13) can be manipulated as follows:

$$\begin{aligned}\mathcal{F}_{1,k}+\mathcal{F}_{1,k}^T \leq&\lambda_{1,k}\Theta_k P_{k|k-1}\Theta_k^T\\ &+\lambda_{1,k}^{-1}K_k\bar{C}_k\mathbb{E}\{\bar{x}_k\bar{x}_k^T\}\bar{C}_k^T K_k^T,\\ \mathcal{F}_{2,k}+\mathcal{F}_{2,k}^T \leq&\lambda_{2,k}\Theta_k P_{k|k-1}\Theta_k^T\\ &+\lambda_{2,k}^{-1}K_k\mathbb{E}\{\sigma(\bar{C}_k\bar{x}_k)\sigma^T(\bar{C}_k\bar{x}_k)\}K_k^T,\\ \mathcal{F}_{3,k}+\mathcal{F}_{3,k}^T \leq&\lambda_{3,k}K_k\bar{C}_k\mathbb{E}\{\bar{x}_k\bar{x}_k^T\}\bar{C}_k^T K_k^T\\ &+\lambda_{3,k}^{-1}K_k\mathbb{E}\{\sigma(\bar{C}_k\bar{x}_k)\sigma^T(\bar{C}_k\bar{x}_k)\}K_k^T.\end{aligned}$$

From Lemma 1, we have

$$\begin{aligned}&\mathbb{E}\{\bar{x}_k\bar{x}_k^T\}\\ =&\mathbb{E}\{(e_{k|k-1}+\hat{x}_{k|k-1})(e_{k|k-1}+\hat{x}_{k|k-1})^T\}\\ \leq&(1+\lambda_{4,k})P_{k|k-1}+(1+\lambda_{4,k}^{-1})\mathbb{E}\{\hat{x}_{k|k-1}\hat{x}_{k|k-1}^T\}.\end{aligned}$$

Recalling the definition of $\sigma_i(\cdot)$ in (5), we have

$$\begin{aligned}&\mathbb{E}\left\{\sigma(\bar{C}_k\bar{x}_k)\sigma^T(\bar{C}_k\bar{x}_k)\right\}\\ \leq&\mathbb{E}\left\{\mathrm{tr}\{\sigma(\bar{C}_k\bar{x}_k)\sigma^T(\bar{C}_k\bar{x}_k)\}\right\}I\\ \leq&\bar{r}I.\end{aligned}$$

Summarizing the above discussions, we have

$$\begin{aligned}P_{k|k} \leq&(1+\lambda_{1,k}+\lambda_{2,k})\Theta_k P_{k|k-1}\Theta_k^T\\ &+(1+\lambda_{1,k}^{-1}+\lambda_{3,k})K_k\bar{C}_k\bar{\Phi}_k\bar{C}_k^T K_k^T\\ &+K_k\big[\bar{r}(1+\lambda_{2,k}^{-1}+\lambda_{3,k}^{-1})I+R_k\big]K_k^T\end{aligned}$$

where

$$\bar{\Phi}_k=(1+\lambda_{4,k})P_{k|k-1}+(1+\lambda_{4,k}^{-1})\mathbb{E}\{\hat{x}_{k|k-1}\hat{x}_{k|k-1}^T\}.$$

Based on the mathematical induction method, we can conclude that $P_{k|k}\leq M_{k|k}$. The proof is now complete.

**Remark 3** *It should be pointed out that it is impossible to obtain the exact value of the estimation error covariance due to the uncertain terms in Lemma 3 such as* $\mathbb{E}\{\sigma(\bar{C}_k\bar{x}_k)\sigma^T(\bar{C}_k\bar{x}_k)\}$. *A feasible yet effective way to get rid of this numerical problem is to establish an upper bound of the estimation error covariance and then minimize such an upper bound by properly designing the estimator gain matrices at each time instant. Moreover, the conservatism of the proposed distributed SE algorithm can be reduced by choosing the scalars* $\lambda_{i,k}$ $(i=1,2,3,4)$ *appropriately.*

Having obtained the upper bound $M_{k|k}$, we are now ready to find the estimator gains with which the upper bound is minimized at each time instant.

Denote $G_k^{(i)}$ as the $i$-th row of the matrix $G_k$, i.e.,

$$G_k^{(i)}\triangleq[G_{i1,k}\ G_{i2,k}\ \cdots\ G_{in,k}]$$

and $M_{k|k-1}^{(i)}$ as the $i$-th row of the block matrix $M_{k|k-1}$. Moreover, we define

$$\begin{aligned}\mathcal{P}_{i,k}\triangleq&(1+\lambda_{1,k}+\lambda_{2,k})H_i\bar{C}_k M_{k|k-1}\bar{C}_k^T H_i\\ &+(1+\lambda_{1,k}^{-1}+\lambda_{3,k})H_i\bar{C}_k\Phi_k\bar{C}_k^T H_i\\ &+H_i\big[\bar{r}(1+\lambda_{2,k}^{-1}+\lambda_{3,k}^{-1})I+R_k\big]H_i,\\ \mathcal{Q}_{i,k}\triangleq&(1+\lambda_{1,k}+\lambda_{2,k})M_{k|k-1}^{(i)}\bar{C}_k^T H_i.\end{aligned}$$

**Theorem 2** *The upper bound of the estimation error covariance* $P_{k|k}$ *can be minimized at each time instant with the state estimator parameter* $G_k=\{G_{ij,k}\}_{n\times n}$ *given by*

$$\begin{cases}G_{ij,k}=0, & a_{ij}=0\\ \bar{G}_k^{(i)}=\bar{\mathcal{Q}}_{i,k}\bar{\mathcal{P}}_{i,k}^{-1}, & a_{ij}\neq 0\end{cases}\tag{17}$$

*where* $\bar{G}_k^{(i)}$ *and* $\bar{\mathcal{Q}}_{i,k}$ *are the simplified matrices by deleting the* $j$*-th* $(j\notin N_i)$ *column from* $G_k^{(i)}$ *and* $\mathcal{Q}_{i,k}$*, respectively. In addition,* $\bar{\mathcal{P}}_{i,k}$ *is a simplified matrix by removing both the* $j$*-th* $(j\notin N_i)$ *row and* $j$*-th* $(j\notin N_i)$ *column from* $\mathcal{P}_{i,k}$.

*Proof:* Taking the trace of (15) yields

$$\begin{aligned}\mathrm{tr}\{M_{k|k}\}=&(1+\lambda_{1,k}+\lambda_{2,k})\mathrm{tr}\{\Theta_k M_{k|k-1}\Theta_k^T\}\\ &+(1+\lambda_{1,k}^{-1}+\lambda_{3,k})\mathrm{tr}\{K_k\bar{C}_k\Phi_k\bar{C}_k^T K_k^T\}\\ &+\mathrm{tr}\big\{K_k\big[\bar{r}(1+\lambda_{2,k}^{-1}+\lambda_{3,k}^{-1})I+R_k\big]K_k^T\big\}.\end{aligned}$$

By resorting to the properties of trace, for $i\neq j$, we have

$$\mathrm{tr}\big\{E_i X E_j^T\big\}=0$$

where $X$ is a matrix with appropriate dimension. Based on the properties of trace, $\mathrm{tr}\{M_{k|k}\}$ can be rewritten as

$$\begin{aligned}&\mathrm{tr}\{M_{k|k}\}\\ =&(1+\lambda_{1,k}+\lambda_{2,k})\Big\{\mathrm{tr}\{M_{k|k-1}\}-2\mathrm{tr}\Big\{\sum_{i=1}^n E_i G_k H_i\\ &\times\bar{C}_k M_{k|k-1}\Big\}+\mathrm{tr}\Big\{\sum_{i=1}^n E_i G_k H_i\bar{C}_k M_{k|k-1}\\ &\times\bar{C}_k^T(E_i G_k H_i)^T\Big\}\Big\}+(1+\lambda_{1,k}^{-1}+\lambda_{3,k})\mathrm{tr}\Big\{\sum_{i=1}^n E_i G_k\\ &\times H_i\bar{C}_k\Phi_k\bar{C}_k^T(E_i G_k H_i)^T\Big\}+\mathrm{tr}\Big\{\sum_{i=1}^n E_i G_k H_i\\ &\times\big[\bar{r}(1+\lambda_{2,k}^{-1}+\lambda_{3,k}^{-1})I+R_k\big](E_i G_k H_i)^T\Big\}.\end{aligned}$$

According to Lemma 2, taking partial derivation of $\mathrm{tr}\{M_{k|k-1}\}$ with respect to $G_k$ and letting the derivative be zero, we have

$$\begin{aligned}&\frac{\partial\mathrm{tr}\{M_{k|k}\}}{\partial G_k}\\ =&-2(1+\lambda_{1,k}+\lambda_{2,k})\Big\{\sum_{i=1}^n E_i M_{k|k-1}\bar{C}_k^T H_i\\ &-\sum_{i=1}^n E_i G_k H_i\bar{C}_k M_{k|k-1}\bar{C}_k^T H_i\Big\}\\ &+2(1+\lambda_{1,k}^{-1}+\lambda_{3,k})\sum_{i=1}^n E_i G_k H_i\bar{C}_k\Phi_k\bar{C}_k^T H_i\\ &+2\sum_{i=1}^n E_i G_k H_i\big[\bar{r}(1+\lambda_{2,k}^{-1}+\lambda_{3,k}^{-1})I+R_k\big]H_i\end{aligned}$$

$$= 0. \tag{18}$$

Subsequently, as $G_k^{(i)}$ represents the $i$-th row of matrix $G_k$, we have

$$G_k^{(i)}\mathcal{P}_{i,k} = \mathcal{Q}_{i,k}.$$

Noting $H_i = \text{diag}\{a_{i1}I \ \cdots \ a_{in}I\}$ and $a_{ij} = 0$ ($j \notin N_i$), we let $\mathcal{P}_{i,k} = \{P_{ab,k}\}_{n\times n}$ and $\mathcal{Q}_{i,k} = \{Q_{b,k}\}_{1\times n}$, then we have

$$\sum_{j=1}^{n} G_{ij,k}P_{jb,k} = Q_{b,k}$$

for $b \in N_i$. As for $b \notin N_i$, the above equation always holds since $P_{jb,k} = Q_{b,k} = 0$. Hence, we can choose $G_{ib,k} = 0$ when $b \notin N_i$ and it can be seen that

$$\bar{G}_k^{(i)}\bar{\mathcal{P}}_{i,k} = \bar{\mathcal{Q}}_{i,k}.$$

Noticing that $\bar{\mathcal{P}}_{i,k} > 0$, $\bar{G}_k^{(i)}$ can be calculated as follows:

$$\bar{G}_k^{(i)} = \bar{\mathcal{Q}}_{i,k}\bar{\mathcal{P}}_{i,k}^{-1}$$

which completes the proof.

**Remark 4** *In the proof of Theorem 2, the sparseness-induced challenge caused by the sensor network topology is tackled by applying the matrix simplification technique proposed in [25]. Different from [25], we have to fully utilize the information from the saturated sensors in the estimator design to guarantee the estimation performance.*

**Remark 5** *Since it is not difficult to verify that the second derivation of* $\text{tr}\{M_{k|k}\}$ *with respect to* $G_k$ *is always positive definite, the estimator gain given by* (17) *is optimal in the sense that the upper bound is minimized.*

**Remark 6** *Up to now, the Kalman-filter-based SE approaches for the online monitoring of the power systems have attracted ever-increasing research attention, see e.g. [13, 29, 30, 41]. As for the online application in the actual power systems, some initial progress has also been reported in [41]. As such, we can find that the online SE for the actual power systems is still at an exploring stage and some efforts are needed to extended the proposed algorithm to the practical large-scale microgrids.*

### *3.2 Performance Analysis*

To facilitate further analysis, the following definition is first introduced.

**Definition 1** *[31] For real numbers* $\mu > 0$, $\varphi > 0$ *and* $0 < \nu < 1$, *if*

$$\mathbb{E}\{\|V(\xi_k)\|^2\} \le \mu\mathbb{E}\{\|V(\xi_0)\|^2\}\nu^k + \varphi$$

*holds for all* $k > 0$, *then the stochastic process* $V(\xi_k)$ *is exponentially bounded in mean square sense.*

For convenience of analysis, we set the weights $a_{ij} = 1$ for $j \in N_i$. The performance analysis of the proposed algorithm is given in the following theorem.

**Theorem 3** *Assume that there exist positive real numbers* $\bar{a}$, $\underline{c}$, $\bar{c}$, $\bar{\phi}$, $\bar{w}$, $\underline{w}$ *and* $\bar{v}$ *such that the following inequalities*

$$\|\bar{A}\| \le \bar{a}, \quad \underline{c} \le \|\bar{C}_k\| \le \bar{c}, \quad \text{tr}\{\Phi_k\} \le \bar{\phi},$$

$$\underline{w}I \le \bar{W}_k \le \bar{w}I, \quad R_k \le \bar{v}I,$$

$$\rho = \bar{a}^2\Big(1 + \frac{n\bar{c}^2}{\underline{c}^2}\Big)^2 < 1 \tag{19}$$

*are satisfied, then the estimation error is exponentially bounded in mean square sense.*

*Proof:* Substituting (10) into (11) and noting that $\Theta_k = I - K_k\bar{C}_k$, we can rewrite $e_{k|k}$ as

$$e_{k|k} = \Theta_k\bar{A}e_{k-1|k-1} + r_k + s_k$$

where

$$r_k = K_k[\bar{C}_k\bar{x}_k - \sigma(\bar{C}_k\bar{x}_k)], \quad s_k = \Theta_k\bar{w}_k - K_k\bar{v}_k.$$

Taking the non-sparse part of $G_k$ into account, it follows from (18) that

$$\sum_{i=1}^{n} E_iG_kH_i = \sum_{i=1}^{n} E_i\Lambda_k\Pi_k^{-1}H_i \tag{20}$$

where

$$\begin{aligned}\Lambda_k &= (1 + \lambda_{1,k} + \lambda_{2,k})M_{k|k-1}\bar{C}_k^T,\\ \Pi_k &= (1 + \lambda_{1,k} + \lambda_{2,k})\bar{C}_kM_{k|k-1}\bar{C}_k^T\\ &\quad + (1 + \lambda_{1,k}^{-1} + \lambda_{3,k})\bar{C}_k\Phi_k\bar{C}_k^T\\ &\quad + \big[\bar{r}(1 + \lambda_{2,k}^{-1} + \lambda_{3,k}^{-1})I + R_k\big].\end{aligned}$$

Recalling the definition $K_k \triangleq \sum_{i=1}^{n} E_iG_kH_i$ and taking the norm for the both sides of (20), we have

$$\|K_k\| \le n\|\Lambda_k\Pi_k^{-1}\| \le n\frac{\bar{c}}{\underline{c}^2} \triangleq \bar{k}.$$

Similarly,

$$\|\Theta_k\| \le 1 + \bar{c}\bar{k} \triangleq \bar{\theta}.$$

Next, it follows from Lemma 1 and (19) that

$$\begin{aligned}&\mathbb{E}\{r_k^Tr_k\}\\ =&\mathbb{E}\big\{[\bar{C}_k\bar{x}_k - \sigma(\bar{C}_k\bar{x}_k)]^TK_k^TK_k[\bar{C}_k\bar{x}_k - \sigma(\bar{C}_k\bar{x}_k)]\big\}\\ \le&(1+\varsigma)\text{tr}\big\{\mathbb{E}\{\bar{x}_k\bar{x}_k^T\}\bar{C}_k^T\bar{K}_k^T\bar{K}_k\bar{C}_k\big\}\\ &+ (1+\varsigma^{-1})\text{tr}\big\{\mathbb{E}\{\sigma(\bar{C}_k\bar{x}_k)\sigma^T(\bar{C}_k\bar{x}_k)\}K_k^TK_k\big\}\\ \le&(1+\varsigma)\bar{c}^2\bar{k}^2\bar{\phi} + (1+\varsigma^{-1})\bar{k}^2m\bar{r} \triangleq \bar{\gamma}\end{aligned}$$

and

$$\begin{aligned}\mathbb{E}\{s_k^Ts_k\} =&\mathbb{E}\{\bar{w}_k^T\Theta_k^T\Theta_k\bar{w}_k\} + \mathbb{E}\{\bar{v}_k^TK_k^TK_k\bar{v}_k\}\\ \le&\bar{\theta}^2nn_x\bar{w} + \bar{k}^2m\bar{v} \triangleq \bar{s}\end{aligned}$$

with $m = \sum_{i=1}^{n} m_i$.

Subsequently, consider the following iterative matrix equation with respect to $\Psi_{k-1}$:

$$\Psi_k = \Theta_k\bar{A}\Psi_{k-1}\bar{A}^T\Theta_k^T + \bar{W}_{k-1} + \varepsilon I \tag{21}$$

with the initial value being $\Psi_0 = \bar{W}_0 + \varepsilon I$ and $\varepsilon > 0$ being a scalar. Then

$$\begin{aligned}\|\Psi_k\| \le&\|\Theta_k\|^2\|\bar{A}\|^2\|\Psi_{k-1}\| + \|\bar{W}_{k-1}\| + \|\varepsilon I\|\\ \le&\rho\|\Psi_{k-1}\| + \bar{w} + \varepsilon\end{aligned} \tag{22}$$

where $\rho$ is defined in (19). By applying the relation (22) recursively, we have

$$\|\Psi_k\| \leq \rho^k \|\Psi_0\| + (\bar{w}+\varepsilon)\sum_{i=1}^{k-1}\rho^i.$$

It follows from $\rho < 1$ that

$$\|\Psi_k\| < \|\Psi_0\| + (\bar{w}+\varepsilon)\sum_{i=1}^{\infty}\rho^i = \|\Psi_0\| + \frac{\bar{w}+\varepsilon}{1-\rho}. \quad (23)$$

Moreover, we can find that

$$\Psi_k \geq \varepsilon I. \quad (24)$$

In view of (23) and (24), there exists a positive scalar $\bar{\psi}$ such that $\varepsilon I \leq \Psi_k \leq \bar{\psi} I$ for $k \geq 0$.

Denote $V_k(e_{k|k}) \triangleq e_{k|k}^T \Psi_k^{-1} e_{k|k}$. For an arbitrary positive scalar $\sigma$, we have

$$\begin{aligned}
&\mathbb{E}\{V_k(e_{k|k})|e_{k-1|k-1}\} - (1+\sigma)V_{k-1}(e_{k-1|k-1}) \\
=&\mathbb{E}\big\{[\Theta_k \bar{A} e_{k-1|k-1} + r_k + s_k]^T \Psi_k^{-1} \\
&\times [\Theta_k \bar{A} e_{k-1|k-1} + r_k + s_k]\big\} \\
&- (1+\sigma) e_{k-1|k-1}^T \Psi_{k-1}^{-1} e_{k-1|k-1} \\
\leq&(1+\sigma)\mathbb{E}\big\{e_{k-1|k-1}^T [\bar{A}^T \Theta_k^T \Psi_k^{-1} \Theta_k \bar{A} - \Psi_{k-1}^{-1}] e_{k-1|k-1}\big\} \\
&+ (1+\sigma^{-1})\mathbb{E}\{r_k^T \Psi_k^{-1} r_k\} + \mathbb{E}\{s_k^T \Psi_k^{-1} s_k\}. \quad (25)
\end{aligned}$$

Resorting to the matrix inversion lemma, we have

$$\begin{aligned}
&\bar{A}^T \Theta_k^T \Psi_k^{-1} \Theta_k \bar{A} - \Psi_{k-1}^{-1} \\
=&\bar{A}^T \Theta_k^T (\Theta_k \bar{A} \Psi_{k-1} \bar{A}^T \Theta_k^T + \bar{W}_{k-1} + \varepsilon I)^{-1} \Theta_k \bar{A} - \Psi_{k-1}^{-1} \\
=&-[I + \bar{A}^T \Theta_k^T (\bar{W}_{k-1} + \varepsilon I)^{-1} \Theta_k \bar{A} \Psi_{k-1}]^{-1} \Psi_{k-1}^{-1} \\
\leq&-\left(1 + \frac{\bar{a}^2 \bar{\theta}^2 \bar{\psi}}{\underline{w}}\right)^{-1} \Psi_{k-1}^{-1}. \quad (26)
\end{aligned}$$

Substituting (26) into (25), we have

$$\begin{aligned}
&\mathbb{E}\{V_k(e_{k|k})|e_{k-1|k-1}\} - (1+\sigma)V_{k-1}(e_{k-1|k-1}) \\
\leq&-(1+\sigma)\left(1 + \frac{\bar{a}^2 \bar{\theta}^2 \bar{\psi}}{\underline{w}}\right)^{-1} V_{k-1}(e_{k-1|k-1}) + \kappa \quad (27)
\end{aligned}$$

with $\kappa = (1+\sigma^{-1})\frac{\bar{\gamma}^2}{\varepsilon} + \frac{\bar{s}^2}{\varepsilon}$. Then, it follows from (27) that

$$\mathbb{E}\{V_k(e_{k|k})|e_{k-1|k-1}\} \leq \chi V_{k-1}(e_{k-1|k-1}) + \kappa$$

where $\chi = (1+\sigma)\Big[1 - \Big(1 + \frac{\bar{a}^2\bar{\theta}^2\bar{\psi}}{\underline{w}}\Big)^{-1}\Big]$. It is obvious that $\chi \in (0,1)$ for some $\sigma > 0$. Accordingly, we have

$$\begin{aligned}
\mathbb{E}\{\|e_{k|k}\|^2\} \leq&\frac{\bar{\psi}}{\varepsilon}\mathbb{E}\{\|e_{0|0}\|^2\}\chi^k + \kappa\bar{\psi}\sum_{i=1}^{k-1}\chi^i \\
\leq&\frac{\bar{\psi}}{\varepsilon}\mathbb{E}\{\|e_{0|0}\|^2\}\chi^k + \kappa\bar{\psi}\sum_{i=1}^{\infty}\chi^i \\
=&\frac{\bar{\psi}}{\varepsilon}\mathbb{E}\{\|e_{0|0}\|^2\}\chi^k + \frac{\kappa\bar{\psi}}{1-\chi}.
\end{aligned}$$

Recalling Definition 1, we can conclude that the estimation error is exponentially bounded in mean square sense.

**Remark 7** *From Theorem 3, it can be concluded that the exponential boundedness in the mean square sense for the estimation error is guaranteed with a sufficient condition. Moreover, the effects caused by the matrix $H_i$ is also reflected in Theorems 2 and 3, which means that the topology information of the sensor network is considered in the estimator design and performance analysis.*

## 4 Simulation Results

In this section, the proposed SE algorithm is tested in a case study of REM which contains two DG units. Consider the sensor network with $n = 4$ sensor nodes, whose topology is represented by a direct graph $\mathcal{G} = (\mathcal{V}, \mathcal{E}, \mathcal{A})$ with $\mathcal{V} = \{1,2,3,4\}$ and

$$\mathcal{A} = \begin{bmatrix} 1 & 0.8 & 0.1 & 0 \\ 0 & 1 & 0.2 & 0 \\ 0 & 0.4 & 1 & 0.2 \\ 0 & 0 & 0.1 & 1 \end{bmatrix}.$$

The parameters of the microgrid with two DG units are shown in Table 1 [33], and the frequency and the sampling time of the microgrid are set as $f_0 = 60$ Hz and $\Delta =$ 1e-5 s, respectively. The measuring items of each sensor node are listed in Table 2. The values of other parameters in the simulation are presented in Table 3, and the saturation levels are all taken as 5. The mean square error (MSE) is used to evaluate the estimation accuracy, i.e., $\text{MSE}_k = \frac{1}{T}\sum_{j=1}^{T}(\bar{x}_k^{(j)} - \hat{x}_{k|k}^{(j)})^T(\bar{x}_k^{(j)} - \hat{x}_{k|k}^{(j)})$ , where $T$ is the number of independent experiments and $T = 100$.

Table 1
Parameters of Simulation Model

| Term | DG unit $r$ | DG unit $s$ |
|---|---|---|
| VSC series filter | $R_{tr} = 1.3$ m$\Omega$ | $R_{ts} = 1.5$ m$\Omega$ |
| VSC series filter | $L_{tr} = 92.6$ $\mu$H | $L_{ts} = 92.6$ $\mu$H |
| Shunt capacitance | $C_r = 62.86$ $\mu$F | $C_s = 76$ $\mu$F |
| Transmission line resistance | $R_{rs} = 1.3$ m$\Omega$ | $R_{sr} = 1.3$ m$\Omega$ |
| Transmission line inductance | $L_{rs} = 600$ mH | $L_{sr} = 600$ mH |
| Transformer ratio Y/$\triangle$ | $d_r = 0.6/13.8$ | $d_s = 0.6/13.8$ |

Table 2
The measuring items of each sensor node

| | |
|---|---|
| $y_{1,k}$ | $[V_{1,r,k}^{ab} \;\; I_{1,tr,k}^{ab} \;\; I_{1,rs,k}^{ab} \;\; I_{1,sr,k}^{ab} \;\; V_{1,s,k}^{ab} \;\; I_{1,ts,k}^{ab}]^T \in \mathbb{R}^{12}$ |
| $y_{2,k}$ | $[V_{2,r,k}^{abc} \;\; I_{2,tr,k}^{ac} \;\; I_{2,rs,k}^{ac} \;\; I_{2,sr,k}^{ac} \;\; V_{2,s,k}^{abc} \;\; I_{2,ts,k}^{ac}]^T \in \mathbb{R}^{14}$ |
| $y_{3,k}$ | $[V_{3,r,k}^{ac} \;\; I_{3,tr,k}^{bc} \;\; I_{3,rs,k}^{bc} \;\; I_{3,sr,k}^{bc} \;\; V_{3,s,k}^{abc} \;\; I_{3,ts,k}^{bc}]^T \in \mathbb{R}^{13}$ |
| $y_{4,k}$ | $[V_{4,r,k}^{ac} \;\; I_{4,tr,k}^{bc} \;\; I_{4,rs,k}^{ac} \;\; I_{4,sr,k}^{ac} \;\; V_{4,s,k}^{abc} \;\; I_{4,ts,k}^{abc}]^T \in \mathbb{R}^{14}$ |

### *4.1 Experiments Under Different Cases*

**Case 1** *Experiments under Sensor Saturations*

In this case, the saturated sensors are considered. Specifically, the saturation levels of $V_r^b$, $I_{tr}^a$, $V_s^c$ and $I_{ts}^c$ are set as 1.2, 1, 1.2 and 1.5, respectively, and the other saturation levels are still chosen as 5. For the sake of saving space, the states $V_r^d$, $I_{tr}^d$, $V_s^d$ and $I_{ts}^d$ (i.e., $x_{1,k}$, $x_{3,k}$,

Table 3
Parameter Values

| Parameter | Value | Parameter | Value |
|---|---|---|---|
| $\Sigma_{0\|0}$ | $\text{diag}_{12}\{0.001\}$ | $W_k$ | $\text{diag}_{12}\{0.1\}$ |
| $R_1(k)$ | $\text{diag}_{12}\{0.25\}$ | $R_2(k)$ | $\text{diag}_{14}\{0.25\}$ |
| $R_3(k)$ | $\text{diag}_{13}\{0.45\}$ | $R_4(k)$ | $\text{diag}_{14}\{0.35\}$ |
| $\lambda_{1,k}$ | 0.5 | $\lambda_{2,k}$ | 0.95 |
| $\lambda_{3,k}$ | 0.2 | $\lambda_{4,k}$ | 0.02 |

$x_{9,k}$ and $x_{11,k}$) are taken for illustration, respectively. The simulation results are plotted in Figs. 2-4, respectively. Specifically, Fig. 2 shows the actual states and their estimates. The curves of the measurements with and without saturations are plotted Fig. 3. Fig. 4 shows the curves of the MSE as well as the upper bound.

From Figs. 2-4, we can find that: 1) the degeneration of the local estimates caused by the sensor saturations can be compensated by using the neighboring sensing information; 2) the proposed DSE scheme improves the overall reliability since some of the local estimates are degraded severely due to the presence of sensor saturations while the other nodes can still track the trajectories of the states accurately; and 3) the performance index is satisfied since the MSE stays below the upper bound.

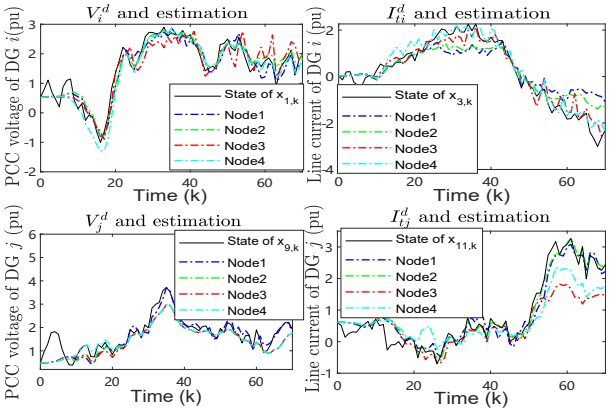


Fig. 2. The estimation results under Case 1.

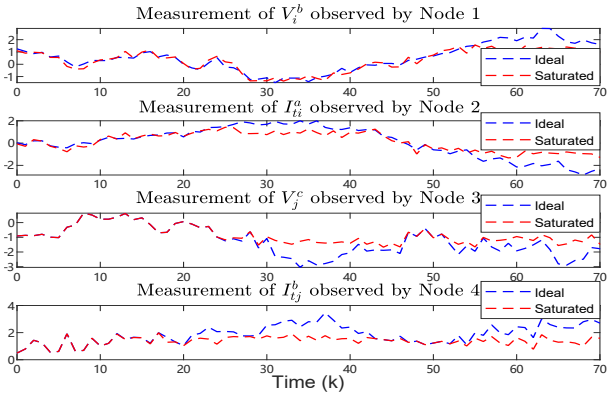


Fig. 3. The measurements with and without saturations.

**Case 2** *Isolated Node Versus the Interacted Node*

In this case, an isolated sensor node which only use its own measurements is considered for the purpose of comparison with our proposed method. For the sake of saving space, the state $x_{11,k}$ estimated by node 1 is taken for illustration. The corresponding results under the saturated sensors are plotted in Fig. 5, where the estimates of $x_{11,k}$ from the interacted node and the isolated node are plotted in the first subfigure, and the second and third subfigures depict, respectively, the absolute value of estimation error of $x_{11,k}$ and the MSE of $x_{11,k}$ after 100 independent experiments. The curves of the measurement $I_{ts}^a$ with and without saturation are plotted in Fig. 6, where the saturation level is set to be 1.9 and the other saturation levels are still chosen as 5.

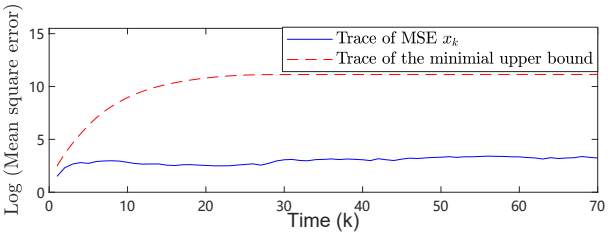


Fig. 4. The MSE and its upper bound under Case 1.

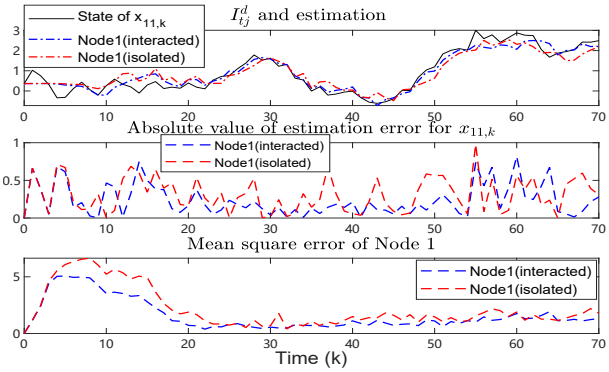


Fig. 5. The estimation results under Case 2.

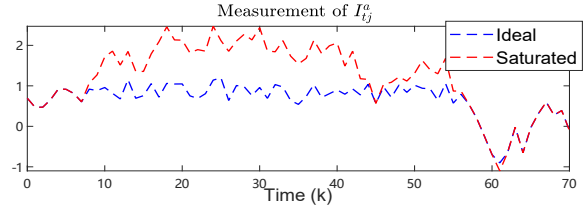


Fig. 6. The measurement with and without saturation.

From Fig. 5, we can find that: 1) when the sensor is not saturated, the deviations of the local estimate can be compensated by using the neighboring information; and 2) the overall reliability of the DSE scheme is higher than the one which uses the local measurements only.

### *4.2 Computational Efficiency*

The proposed algorithm is tested in MATLAB R2018b. All the test cases are performed on a PC with Intel Core CPU i7-7700HQ, 2.80GHz and 16 GB RAM. The average computing time of our proposed algorithm for each time step is 1.82 ms, which is much lower than the PMU update rate (16.7 ms) reported in [41]. Therefore, the proposed algorithm is suitable for online application.

## 5 Conclusion

In this paper, the DSE problems has been investigated for REM with sensor saturations. The explicit model of microgrid with sensor saturations has been proposed.

The distributed recursive estimator proposed in this paper has guaranteed an upper bound of the estimation error covariances, and the estimator gain matrices have been designed by minimizing such an upper bound at each time instant. Moreover, in order to ensure that the estimation error is exponentially bounded in the mean square sense, a sufficient condition has been conducted. Finally, a simulation based on the model of REM has been provided to verify the performance of the proposed distributed scheme. The simulation results have demonstrated that the developed SE scheme is effective.

## References


[1] Ahmad, F., Rasool, A., Ozsoy, E., Rajasekar, S., Sabanovic, A., & Elitas, M. (2018). Distribution system state estimation–A step towards smart grid. *Renewable & Sustainable Energy Reviews*, *81*, 2659–2671.

[2] Basin, M. V., Loukianov, A. G., & Hernandez-Gonzalez, M. (2013). Joint state and parameter estimation for uncertain stochastic nonlinear polynomial systems. *International Journal of Systems Science*, *44*(7), 1200–1208.

[3] Caballero-Águila, R., Hermoso-Carazo, A., & Linares-Pérez, J. (2017). Distributed fusion filters from uncertain measured outputs in sensor networks with random packet losses. *Information Fusion*, *34*, 70–79.

[4] D. Chen, W. Chen, J. Hu and H. Liu, Variance-constrained filtering for discrete-time genetic regulatory networks with state delay and random measurement delay, *International Journal of Systems Science*, vol. 50, no. 2, pp. 231–243, 2019.

[5] Chen, L., Yue, D., Dou, C., Cheng, Z., & Chen, J. (2020). Robustness of cyber-physical power systems in cascading failure: Survival of interdependent clusters. *International Journal of Electrical Power & Energy Systems*, https://doi.org/10.1016/j.ijepes.2019.06.032.

[6] Y. Chen, Z. Wang, Y. Yuan and P. Date, Distributed $H_\infty$ filtering for switched stochastic delayed systems over sensor networks with fading measurements, *IEEE Transactions on Cybernetics*, vol. 50, no. 1, pp. 2–14, 2020.

[7] Cheng, Z., Yue, D., Hu, S., Huang, C., Dou, C.,& Chen, L. (2020). Resilient load frequency control design: DoS attacks against additional control loop. *International Journal of Electrical Power & Energy Systems*, https://doi.org/10.1016/j.ijepes.2019.105496.

[8] Choi, S. & Meliopoulos, A. P. (2017). Effective real-time operation and protection scheme of microgrids using distributed dynamic state estimation. *IEEE Transactions on Power Delivery*, *32*(1), 504–514.

[9] Ciuonzo, D., Aubry, A., & Carotenuto, V. (2017). Rician MIMO channel- and jamming-aware decision fusion. *IEEE Transactions on Signal Processing*, *65*(15), 3866–3880.

[10] Dehghanpour, K., Wang, Z., Wang, J., Yuan, Y., & Bu, F. (2019). A survey on state estimation techniques and challenges in smart distribution systems. *IEEE Transactions on Smart Grid*, *10*(2), 2313–2322.

[11] El-Sharafy, M. Z., Saxena, S., & Farag, H. E. (2019). Optimal design of islanded microgrids considering distributed dynamic state estimation. *IEEE Transactions on Industrial Informatics*, *17*(3), 1592–1603.

[12] Francy, R. C., Farid, A. M., & Youcef-Toumi, K. (2015). Event triggered state estimation techniques for power systems with integrated variable energy resources. *Isa Transactions*, *56*, 165–172.

[13] Ghahremani, E. & Kamwa, I. (2011). Online state estimation of a synchronous generator using unscented Kalman filter from phasor measurements units. *IEEE Transactions on Energy Conversion*, *26*(4), 1099–1108.

[14] Ghiga, R., Martin, K., Wu, Q., & Nielsen, A. H. (2018). Phasor measurement unit test under interference conditions. *IEEE Transactions on Power Delivery*, *33*(2), 630–639.

[15] J. Hu, Z. Wang, G.-P. Liu, H. Zhang and R. Navaratne, A prediction-based
approach to distributed filtering with missing measurements and communication delays through sensor networks, *IEEE Transactions on Systems, Man, and Cybernetics: Systems*, in press, DOI: 10.1109/TSMC.2020.2966977.

[16] Hu, L., Wang, Z., Liu, X., Vasilakos, A. V., & Alsaadi, F. E. (2017). Recent advances on state estimation for power grids with unconventional measurements. *IET Control Theory and Applications*, *11*(18), 3221–3232.

[17] Huang, Y.-F., Werner, S., Huang, J., Kashyap, N., & Gupta, V. (2012). State estimation in electric power grids: Meeting new challenges presented by the requirements of the future grid. *IEEE Signal Processing Magazine*, *29*(5), 33–43.

[18] IEEE Standard 1547.1-2005. IEEE Standard Conformance Test Procedures for Equipment Interconnecting Distributed Resources with Electric Power Systems.

[19] Jena, P. & Pradhan, A. K. (2016). Reducing current transformer saturation effect in phasor measurement unit. *International Transactions On Electrical Energy Systems*, *26*(7), 1397–1407.

[20] Kommuri, S. K., Defoort, M., Karimi, H. R., & Veluvolu, K. C. (2016). A robust observer-based sensor fault-tolerant control for PMSM in electric vehicles. *IEEE Transactions on Industrial Electronics*, *63*(12), 7671–7681.

[21] Krause, P., Wasynczuk, O., Sudhoff, S. D., & Pekarek, S. (2013). *Analysis of Electric Machinery and Drive Systems*. Wiley-IEEE Press.

[22] Li, J., Liu, H., Martin, K. E., Li, J., Bi, T., & Yang, Q. (2019). Electronic transformer performance evaluation and its impact on PMU. *IET Generation Transmission & Distribution*, *13*(23), 5396–5403.

[23] Q. Li, B. Shen, Z. Wang and W. Sheng, Recursive distributed filtering over sensor networks on Gilbert-Elliott channels: A dynamic event-triggered approach, *Automatica*, vol. 113, art. no. 108681, 2020.

[24] X. Li, F. Han, N. Hou, H. Dong and H. Liu, Set-membership filtering for piecewise linear systems with censored measurements under Round-Robin protocol, *International Journal of Systems Science*, vol. 51, no. 9, pp. 1578–1588, Jul. 2020.

[25] Liu, Q., Wang, Z., He, X., Ghinea, G., & Alsaadi, F. E. (2017). A resilient approach to distributed filter design for time-varying systems under stochastic nonlinearities and sensor degradation. *IEEE Transactions on Signal Processing*, *65*(5), 1300–1309.

[26] Y. Liu, Z. Wang, L. Ma and F. E. Alsaadi, A partial-nodes-based information fusion approach to state estimation for discrete-time delayed stochastic complex networks, *Information Fusion*, vol. 49, pp. 240–248, Sept. 2019.

[27] L. Ma, Z. Wang, C. Cai and F. E. Alsaadi, A dynamic event-triggered approach to $H_\infty$ control for discrete-time singularly perturbed systems with time-delays and sensor saturations, *IEEE Transactions on Systems, Man, and Cybernetics: Systems*, in press, DOI: 10.1109/TSMC.2019.2958529.

[28] W. Qian, Y. Li, Y. Chen, and W. Liu, $L_2$-$L_\infty$ filtering for stochastic delayed systems with randomly occurring nonlinearities and sensor saturation, *International Journal of Systems Science*, vol. 51, no. 13, pp. 2360–2377, 2020.

[29] Qu, B., Li, N., Liu, Y., & Alsaadi, F. E. (2020). Estimation for power quality disturbances with multiplicative noises and correlated noises: A recursive estimation approach. *International Journal of Systems Science*, *51*(7), 1200–1217.

[30] Qu, B., Wang, Z., & Shen, B. (2021). Fusion estimation for a class of multi-rate power systems with randomly occurring SCADA measurement delays. *Automatica*, https://doi.org/10.1016/j.automatica.2020.109408.

[31] Reif, K., Gunther, S., Yaz, E., & Unbehauen, R. (1999). Stochastic stability of the discrete-time extended Kalman filter. *IEEE Transactions on Automatic Control*, *44*(4), 714–728.

[32] Rana, M. M., Li, L., Su, S. W., & Xiang, W. (2018). Consensus-based smart grid state estimation algorithm. *IEEE Transactions on Industrial Informatics*, *14*(8), 3368–3375.

[33] Riverso, S., Sarzo, F., & Ferrari-Trecate, G. (2015). Plug-and-play voltage and frequency control of islanded microgrids with meshed topology. *IEEE Transactions on Smart Grid*, *6*(3), 1176–1184.

[34] Schweppe, F. C. & Wildes, J. (1970). Power system static-state estimation, part I, II and III. *IEEE Transactions on Power Apparatus and Systems*, *PAS-89*(1), 120–135.

[35] Y. Shen, Z. Wang, B. Shen and F. E. Alsaadi, $H_\infty$ filtering for multi-rate multi-sensor systems with randomly occurring sensor saturations under the p-persistent CSMA protocol, *IET Control Theory and Applications*, vol. 14, no. 10, pp. 1255–1265, 2020.

[36] J. Song, D. Ding, H. Liu and X. Wang, Non-fragile distributed state estimation over sensor networks subject to DoS attacks: The almost sure stability, *International Journal of Systems Science*, vol. 51, no. 6, pp. 1119–1132, Apr. 2020.

[37] Tuballa, M. L. & Abundo, M. L. (2016). A review of the development of smart grid technologies. *Renewable & Sustainable Energy Reviews*, *59*, 710–725.

[38] Tan, H., Shen, B., Peng, K., & Liu, H. (2020). Robust recursive filtering for uncertain stochastic systems with amplify-and-forward relays. *International Journal of Systems Science*, *51*(7), 1188–1199.

[39] Wen, C., Wang, Z., Geng, T., & Alsaadi, F. E. (2018). Event-base distribute recursive filtering for state-saturated systems with redundant channels. *Information Fusion*, *39*, 96–107.

[40] Zhang, C.-K., Jiang, L., Wu, Q. H., He, Y., & Wu, M. (2013). Delay-dependent robust load frequency control for time delay power systems. *IEEE Transactions on Power Systems*, *28*(3), 2192–2201.

[41] Zhao, J. & Mili, L. (2019). Power system robust decentralized dynamic state estimation based on multiple hypothesis testing. *IEEE Transactions on Power Systems*, *33*(4), 4553–4562.

[42] Z. Zhao, Z. Wang, L. Zou and J. Guo, Set-Membership filtering for time-varying complex networks with uniform quantisations over randomly delayed redundant channels, *International Journal of Systems Science*, vol. 51, no. 16, pp. 3364–3377, 2020.

[43] L. Zou, Z. Wang, Q.-L. Han and D. H. Zhou, Recursive filtering for time-varying systems with random access protocol, *IEEE Transactions on Automatic Control*, vol. 64, no. 2, pp. 720–727, 2019.

[44] L. Zou, Z. Wang and D. H. Zhou, Moving horizon estimation with non-uniform sampling under component-based dynamic event-triggered transmission, *Automatica*, vol. 120, art. no. 109154, 2020.

[45] L. Zou, Z. Wang, Q.-L. Han and D. H. Zhou, Full information estimation for time-varying systems subject to Round-Robin scheduling: A recursive filter approach, *IEEE Transactions on Systems, Man, and Cybernetics: Systems*, in press, DOI: 10.1109/TSMC.2019.2907620.